Nat. Volatiles & Essent. Oils, 2021; 8(5): 1773 - 1784

NVEO
Natural Volatiles &
Essential Oils

Using GPS and LASER optic position determination system for detailed visual recognition in mobile robot guidance

[1]Dr. Dinesh.G, [2]Dr. Anandakumar Haldorai, [3]Dr. P. Suresh, [4]Mr. Robert Theivadas J, [5]Dr.Ram Subbiah, [6]Dr. S. Lakshmi narayanan

1 Sr. Assistant Professor, New Horizon College Of Engineering, Outer Ring Road, Kadubeesanahalli, Bengaluru-560 103, Karnataka. dineshcsenhce@gmail.com
2 Professor (Associate), Department of Computer science and engineering,
Sri Eshwar College of Engineering, Coimbatore, Tamil Nadu, India, 641202. anandakumar.psgtech@gmail.com
3 Dept of ECE, Veltech Rangarajan Dr Sagunthala R and D Institute of Science and Technology, Chennai, Tamilnadu, India. suresh3982@yahoo.co.in
4 Director, Digialtyic Technologies, Chennai, Tamilnadu, India. Robert@digialtyic.com
5 Associate Professor, Mechanical engineering, Gokaraju Rangaraju institute of Engineering and Technology, Hyderabad. ram4msrm@gmail.com
6 Associate Professor, Department of ECE, Gojan school of Buisness and Technology, Chennai. s.lakshminarayanan@gojaneducation.com

Abstract:

Mobile robots have played an important part in the army, industry, and farming applications. The mobile robot must travel the desired path while avoiding obstacles along the way. Many scientists have found solutions by utilizing various types of controlling and instrumentation systems. The intricacy of mobile robot devices might turn them expensive and risky. A mobile robot having GPS tracking and obstacle detection is suggested, using a cheap mobile frame, sonar sensor, and GPS module. The mobile robot's positioning and obstacle detection will be determined using a mix of sonar and GPS. The mobile robot must move corresponding to this GPS device's waypoints, as well as the sonar sensor identifies obstacles throughout the robot navigating by activating the sonar sensor through succession via the controlled loop daisy-chaining application technique. We have created a device to detect the location and postures of mobile robots even under channels and flyovers in areas with low floors. It is quite simple to set up a system that employs laser projection pointers and cameras. An image application computed the location and postures of the cameras and mobile robot after photographing a targeted structure and projecting laser pointers.

Index terms—Global positioning system (GPS), LASER, robot positioning, visual recognition.

1. Introduction

A self-contained device which does no longer requires human involvement to operate is an autonomous mobile robot. Even before the procedure, all moves are planned, and the mobile robot would travel properly. Autonomous mobile robots may be classified into three types of environments: ground, air, and underwater. The use of autonomous mobile robots is with the army, farming, security, as well as other applications can reduce the danger of damage and save time. Many academics are devoting significant effort and resources to the development of such an autonomous mobile robot. The Military applications used for explosive defusing have a significant influence on reducing fatal injuries. In another area such as military could employ autonomous mobile robots to rescue wounded soldiers from conflict. Another use for military objectives is autonomous mobile de-mining robots [1]. Several of those applications can save lives and are appropriate for today's unforeseen conflict.

A conceivable objective for Autonomous Mobile Robot would be to move from location to location along a pre-programmed path with avoiding obstacles. This function may be used in systems including autonomous log skidder, robot camera for surveillance, a fire protection system, and a topography vehicle. This duty can be accomplished by the vehicles employing sensors that could "see" where it stands and whatever is nearby it. Such sensors span from short infrared sensors via long-range high-frequency waves and GPS satellites [2].

Several sensors are available to help a mobile robot determine its very own location. Robots that move outside use a famous sensor known as the Global Positioning System (GPS). Measures for GPS-enabled robots have recently been demonstrated to be increasingly precise as GPS location accuracy has advanced. Furthermore, GPS is ineffective in locations with high floors, like caves and flyovers. The stereo-camera approaches [3] and architecture from movement [4] are two techniques for supplementing GPS. A variety of image-processing methods are still in widespread use [5-7]. These are successful approaches since they do not require an external connection and could estimate a location from simply an image [8-10]. Image processing is also used to assess architecture [11-14]. Furthermore, contain two issues: "occlusion" and the correlation of certain pictures. The identical point must be maintained in multiple pictures created during parallax, however, the associated point on the image became problematic when every alternative image isn't clearly distinguished from the measuring topic.

LRF is efficient at gathering 3D data over a large area, although its budget with point group processing seems prohibitively expensive. LRF (laser rangefinder) is indeed an example of a non-measuring instrument method [15]. Lasers and cameras combine to make LRF. Mirrors alter the irradiated edges, as well as the laser can irradiate a certain spot mostly on measuring subject. The coordinates of such a point are correlated in 3D, as well as irradiance of the measuring item is triangulated by the laser's location, the irradiated edge, the angle is computed in the LRF and in-camera location. Furthermore, since it is essentially a point measuring, a scanner technique is required to travel the irradiated point across the entire item, which is required to get 3D shape knowledge of the entire object. Furthermore, mirror surfaces covered with, say, metal goods have potentially unmeasurable properties. RGB-d cameras may concurrently analyze the intensity and visual images utilizing TOF (time-of-flight measurement), as well as RGB-d cameras, may acquire extensive data to make 3D modeling that can enable the measuring of a particular object. Several research is conducted on the self-positioning of a given mobile robot that has been done with an RGB-d camera [16-18].

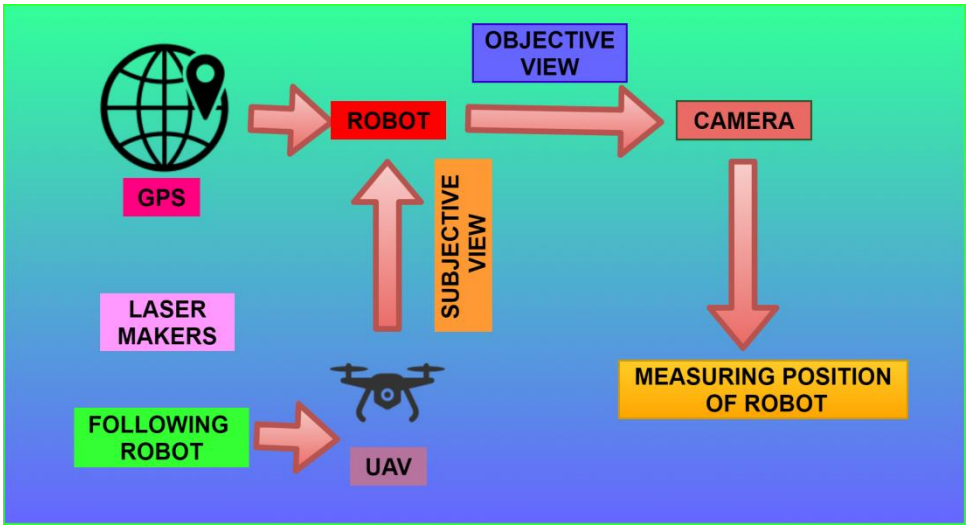

Figure 1: The proposed optic position determination.

We created a method that uses laser projection indicators to detect the location and postures of infrastructure inspection robots. Shown Figure 1 depicts our device's idea. This may be used to calculate the relative location and postures throughout the projection plane. We attempt to determine the location and postures of camera 1 based on its actual perspective. A camera is attached to a laser pointer which irradiates throughout the path of the image, but such a camera is used to estimate the comparative location of the item by capturing a reflected marker.

The camera and laser projection maker are set up which is quite easy. Image application computes the camera's and mobile robot's location and posture where the camera photographs on a destination structure. Unlike the conventional landmark technique, this solution doesn't require the installation of a marker in the surroundings. RGB-d necessitates the pairing of visual and distant images, which might result in computing mistakes. Contrary, because our technique is dependent solely on the optical picture of the targeted surface produced either by laser, then there exists no similarity between various information and no inaccuracy in the interior factors. This can minimize the quantity of data necessary and increase speed execution. The technology improves the effectiveness of building examinations and reduces examination time.

2. State-of-the-art

The major navigating sensor modalities utilized for automobile guiding, navigating, and controlling is defined as the Global Positioning System. Furthermore, a detailed investigation known as the Volpe report [19] identifies many GPS hazards related to signal interruptions. The Volpe Report categorizes GPS signal disturbance into two types: inadvertent and purposeful interruptions. Ionosphere interference (commonly called the ionospheric scintillation), the other one RF interference (public television, mobile phones, including 2-way pagers) are examples of inadvertent interruptions, while jamming, spoofed, are examples of deliberate interruptions.

A few of the study's final suggestions were to "raise knowledge of the necessity for GPS storage systems by many participants of the regional and worldwide road transport society" and to "execute a thorough assessment of GPS standby route planning," which consists of instrument landing systems (ILS), an inertial navigation systems(INS) and long-range navigation (LORAN) [19].

The Volpe study sparked a quest for methods to address the flaws in the present GPS navigational system. Almost majority of the resultant techniques used the proposed GPS backups techniques, which return to archaic/legacy approaches. Consequently, the extent of such navigating modality is restricted by the cost of their ground transmitter, which is prohibitively pricey in remote, dangerous, or hostile settings. Depending on these constraints, scientists have looked at local techniques of determining location whenever GPS is unavailable. Because of improvements in technology vision, estimations, control theory, and monocular camera systems have grown in popularity as a local alternative. One barrier to using a vision device as a navigating aide is the challenge in recreating inertial values from the displayed picture. The mobility of featured elements in an image is used in current techniques to estimate the aircraft condition using a camera system.

A geometrical technique is suggested (with early findings [20, 21]) that estimates location and direction concerning such an inertial posture via a set of homograph connections. This method generates a succession of "daisy-chained" posture estimations (refer [22, 23]), wherein the current local features are linked to already seen feature points that establish the present coordinates on each. Through such connections, already recorded GPS information may be combined with picture information to give location estimations in navigational areas wherever GPS is not available. The technique also provides a precise estimate of vehicle attitude, which would be a known issue in aerial vehicle management. The positioning and angle (i.e., pose) estimate technique may be used in actual time, trying to make it suitable for application in airplane closed-loop guiding management. In the previous decade, there's been a lot of interest in the notion of vision-based management for a flying vehicle. Current literature on a vision-based status estimate for application in flying vehicle control may be divided into many categories.

One contrast is that certain techniques need concurrent sensor fusion [24, 25], whilst others depend simply on camera input [26]. Methods that need prior information of benchmarks (such as design or form [27 &28], the light intensity changes [29], and runway boundaries or lights [30, 31]) are distinguished from approaches that do not require any previous understanding of benchmarks [32, 33 &34]. Techniques that need picture characteristics to stay in the field of view [35] are yet another topic of study, as are techniques capable of capturing new characteristics [36]. Lastly, techniques for information retrieval may be classified depending upon on vision-based methodology used, also including optic flow [37], the simultaneous localization and mapping (SLAM) [38, 39], a stereo vision [40], otherwise epi polar geometry [33, 41, &42]. This final group might potentially be divided into techniques that are highly expensive and hence indicate the amount of actual, onboard computing viability.

Caballero et al. [24] and the Shakernia et al. [14] offer techniques for estimating an airplane's posture via homograph connections between pictures (known simply as a "planar essential matrix"). Caballero et al approaches are described in detail below.is restricted to fly over a flat area, but this approach generates an image mosaic, that could be memory intensive. Shakernia's method ignores characteristic points that enter and depart the camera's field of view. In comparison to earlier approaches [9—13], the technique described here is geared for usage with a static wing airplane, thus it expressly collects fresh characteristic points whenever the present elements risk exiting the picture, and no goal model is required. Flight over even a stable planar area is additionally loosened to enable flight across piece-wise planar patchwork, which would be more typical in real-world circumstances.

3. Systematic Approach

In guidance and positioning, the Global Positioning Systems (GPS) are frequently used. Several robots are nowadays fitted with GPS systems that allow them to navigate to their desired destination. With the use of time as well as other information like heading, the GPS user may estimate the path they should take. The utilization of data transmitted from a satellite to a GPS device will be aided by this effort. For such a purpose, the automated mobile robot will employ a Garmin E-Trex Vista GPS device. This application has been given a lot of thought. A 12 channel GPS receiver, which operates on the L1 frequency, is the most important aspect to examine. This GPS receiver constantly monitors and utilizes the signal to calculate as well as update location. Because of its tiny size, it is simple and comfortable to use, and the waterproofing allows it to be used in rough terrain. It's also appropriate for autonomous mobile robots that demand more power for localization and navigation due to the minimum power requirement of 3v. The precision will then be ± 2 with ± 5 degrees excessive north and south latitude as well as 1-degree precision with correct validation. $GPRMC, $GPRMB, $$GPGGA, as well as HCHDG are the signals from the GPS which are appropriate for guidance and positioning. Latitude and longitude, as well as bearing, are all GPS information used in this research. A predetermined waypoint can also be set, as well as the automated mobile robot will continue that path. All of the data will be received as ASCII code, which will require to be parsed into different types of information. The GPS module's precision can generally be up to 9 meters.

According to the rule below, the mobile robot will move through the desired location as illustrated in Figure 2:

Let’s

True Course=Heading = TR

Waypoint Heading = WP

If WP>TR Move RIGHT

If TR>WP Move LEFT

If TR=WP Move FORWARD

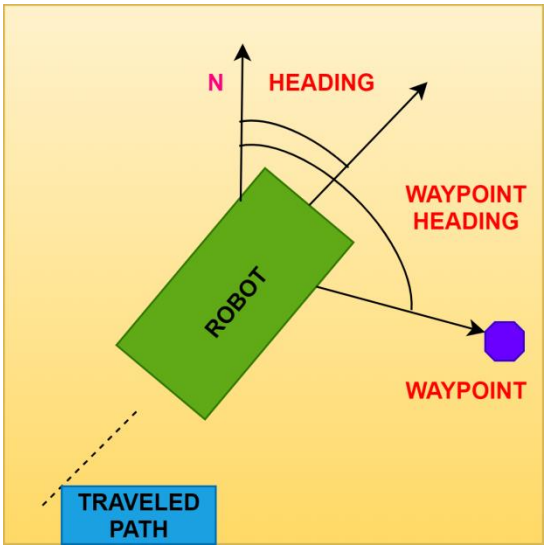

Figure 2: Mobile robot navigation.

3.1. Obstacle Avoidance

The impediment within proximity will be detected by the ultrasonic sensor as the guidance progresses from the initial to an ultimate destination. The primary idea of mobile robot navigation is to minimize obstacles, and once the impediment has been successfully avoided, the mobile robot will adjust the destination from its current location. Using LV-MAX Sonar for avoiding obstacles was the subject of this research. The LV-MAX Sonar requirement is used to determine which sonar sensor to use. This LV-MAX Sonar provides a cheaper sonar detector with dependable and consistent date information, as well as a quick measuring cycle. For avoiding obstacles, four sonar detectors have been installed in front of the automated robot. Every left, as well as right sensor, is 20 cm apart with a 45-degree inclination, and there are two sonar sensors in the center of every left and right sonar detector with a distance of 10 cm among them. Both left and right sensors will recognize the barrier on either side of the automated robot, while the central sensor will recognize the barrier on the opposing end. Since mobile robots only move left and right to eliminate obstacles, the device did not contain a backside sensor. This research used pulse width outcomes to output information from the sonar detector. Equations (1) and (2) can be used to translate pulse values to centimeters or inches.

$$Distance(cm) = \frac{\#microsecond}{29} \quad (1)$$

$$Distance(inches) = \frac{\#microsecond}{74} \quad (2)$$

3.2. The Measurement System Model Using Projection Laser Markers:

A camera was attached to such a laser marker which was shined in the path of the capture, so this camera was used to capture a reflective marker to calculate the comparative location of the objects. Camera 1 may picture the projecting laser pointers of Camera 2 as well as all other things. Every camera's and laser beams' location and attitude relationships are recorded. The projecting laser pointers were formed when every laser beam passed the targeted projecting line markers. The universal coordinate system for Camera 1 seems to be $X_{c1} - Y_{c1} - Z_{c1}$, and the universal coordinate system for Camera 2 is $X_{c2} - Y_{c2} - Z_{c2}$,. The projecting plate's coordinates system seems to be

$X_{pl} - Y_{pl} - Z_{pl},$. A translation expresses the location and stance of every regional coordinates system, the turning of Camera 1's system of coordinates as well as universal coordinate systems. The basis of a plane's coordinate framework is now on the z-axis of Camera 1's coordinate's framework, therefore the stance of the Z_{pl}-axis perimeter can be neglected in this concept since this targeted projecting plate is believed to be infinite.

To determine the location and attitude of camera 2 from such an image from camera 1, the accompanying characteristics were computed: $Z_{pl-c1}, \theta_{xpl}, \theta_{ypl}$ are targeted projecting plate, Camera 1 and Camera 2's comparative stances: $x_{c2-c1}, y_{c2-c1}, z_{c2-c1}$, Camera 2 stance: $\theta_{xc2}, \theta_{yc2}, \theta_{zc2}$

The following are the subscript descriptions of variables. $C_i(i = 1,2)$: camera i, pl: targeted projecting plate, $LA_m(m = 1{\sim}5)$: laser marker $m, n(= 1,2)$: the number of any location upon on laser, PR: projecting position of laser, pro: prediction point upon on imaging plane. The focal length is denoted by the letter f. The image sensor's size is given by h.

To determine the comparative location and attitude among two cameras using the projecting plate, we initially determine the comparative location and attitude among every camera as well as the projecting plate, and afterward the comparative location and attitude among the cameras. The equations of the projecting plane are calculated from coordinates of the three projected points of a laser marker during the first assessment by "Topic view," as well as the comparative positioning attitude among the camera as well as the projecting plane is determined from every parameter of a formula.

3.3. Measurements from the camera image, the location of the Projected Laser Pointer: 'Subject View'

The comparative location and attitude of a camera as well as the objective projecting plate will be determined in this part. Our ultimate goal is to create an actual view modeling that uses projecting laser pointers on the targeted projecting plate to determine the comparative location and attitude of every camera. But, before we look at the actual view modeling, we look at the subjective view concept, which estimates the location of the projecting laser pointer from the image taken. Camera 1, is used to assess the subjective view, so it features three laser markers. The geometrical relationship among the cameras and laser markers was established, as well as three laser markers were displayed on the targeted projecting plate to determine the camera's comparative location and attitude. The targeted projecting plate's location was estimated using the measurements of three projecting laser pointers on the targeted projecting plates. The three laser markers' axes are parallel to a camera's optical axis in this study. The location coordinates of a camera's three projecting laser pointers are used to determine the comparative location and attitude among the camera as well as the targeted projecting plate.

Using a vector of such a spot on a laser beam from camera 1, and a positional vector of projecting point, conversion from the visual plane of Camera 1 to Camera 2 is described as follows.

$$c1_{p_{(1\ \ m)}\ -c1} = \begin{pmatrix} x_{LA\ \ (1\ m\ n)\ -c1} \\ y_{LA\ \ (1\ m\ n)\ -c1} \\ \dfrac{f.x_{LA\ (1\ m\ n)\ -c1}}{h.u_{PRpro\ (1\ m)\ -c1}} \end{pmatrix} = \begin{pmatrix} x_{LA\ (1\ m\ n)\ -c1} \\ y_{LA\ (1\ m\ n)\ -c1} \\ z_{LA\ (1\ m\ n)\ -c1} \end{pmatrix} \quad (3)$$

Calculations of the targeted projecting plate are computed using location coordinates of a three laser marker on the targeted projecting plate to produce the relative location and attitude among a camera as well as the targeted projecting plate. The outside products of such two-directional vector coordinates represented in Camera 1's camera coordinate scheme are found. A standard aspect vector is produced by the exterior product of a directional vector. As a result, the elements of the equation for the targeted projecting plate are the values of such a typical vector. A unitary vector of the destination projecting plate's normal vector is represented as following using the amplitude of a normalized vector $|\overrightarrow{n_{PR}}|$:

$$\frac{\overrightarrow{n_{PR}}}{|\overrightarrow{n_{PR}}|} = \frac{1}{\sqrt{{a_{PR}}^2+{b_{PR}}^2+{c_{PR}}^2}}\begin{pmatrix} a_{PR} \\ b_{PR} \\ c_{PR} \end{pmatrix} = \begin{pmatrix} x_{nePR} \\ y_{nePR} \\ z_{nePR} \end{pmatrix} \quad (4)$$

Using the above equation, comparative stance θ_{xpl}, θ_{ypl} is stated as follows:

$$\theta_{xpl} = arcsin\left(-\frac{y_{nePR}}{cos\theta_{ypl}}\right), \theta_{ypl} = \arcsin\left(x_{nePR}\right) \quad (5)$$

4. Result and discussion

Figure 3 shows a graph of latitude data from $GPGGA, which was acquired well before guidance to check the GPS module's reliability. A total of 400 data points have been collected. Within 300 datasets, all of the data points begin with a similar value, indicating that the latitude significance is appropriate to be utilized for guidance. Figure 4 depicts a graph of longitude with latitude.

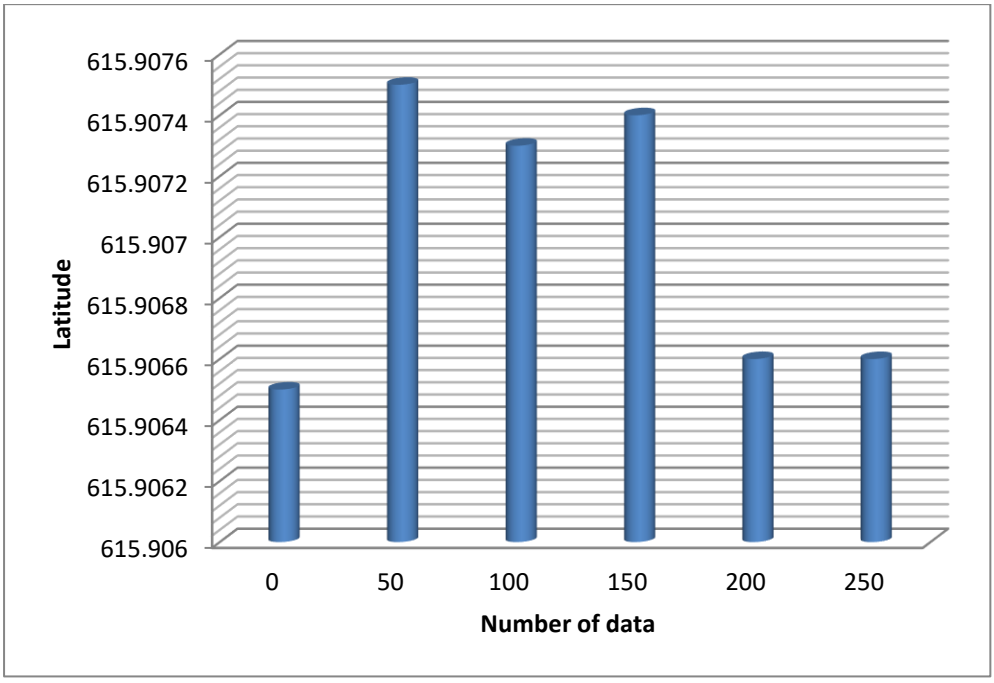

Figure 3: Latitude versus Number of data.

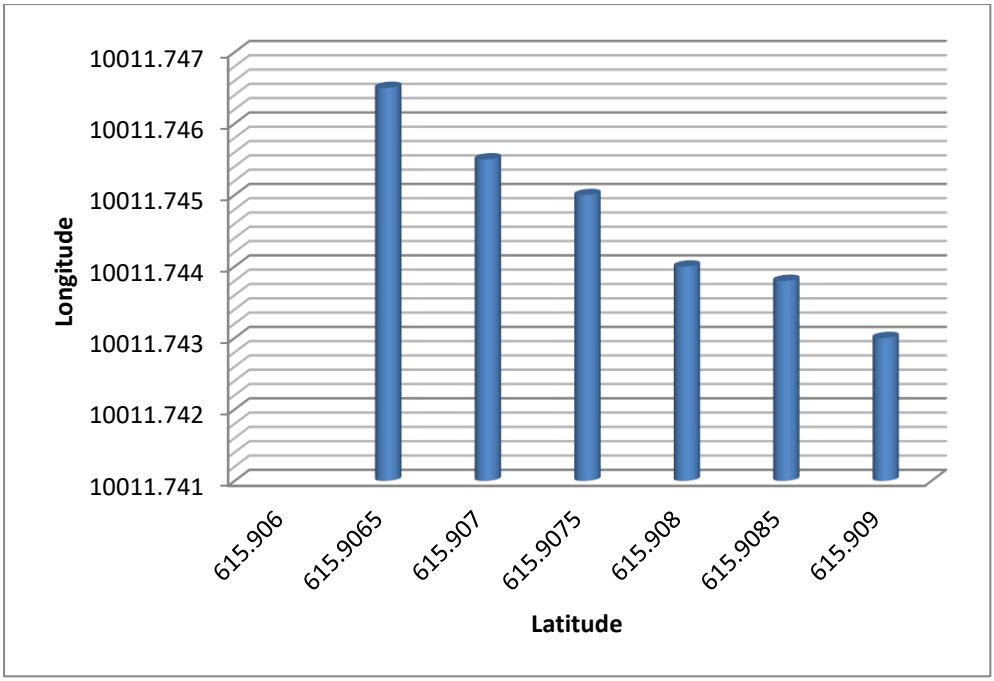

Figure 3: Latitude versus Longitude.

Figure 5 depicts the results of positioning measurements by topic viewpoint. The highest positional inaccuracy of 2.8 percent was recorded. As in the range of firing distances from 1000 to 4000 mm, this device could detect locations with such an inaccuracy of lower than 50 mm. Moreover, since the picture quality per pixel dropped as the measuring distance extended, the measuring location inaccuracy within the range of firing range from 5000 to 7000 mm is about 50 mm.

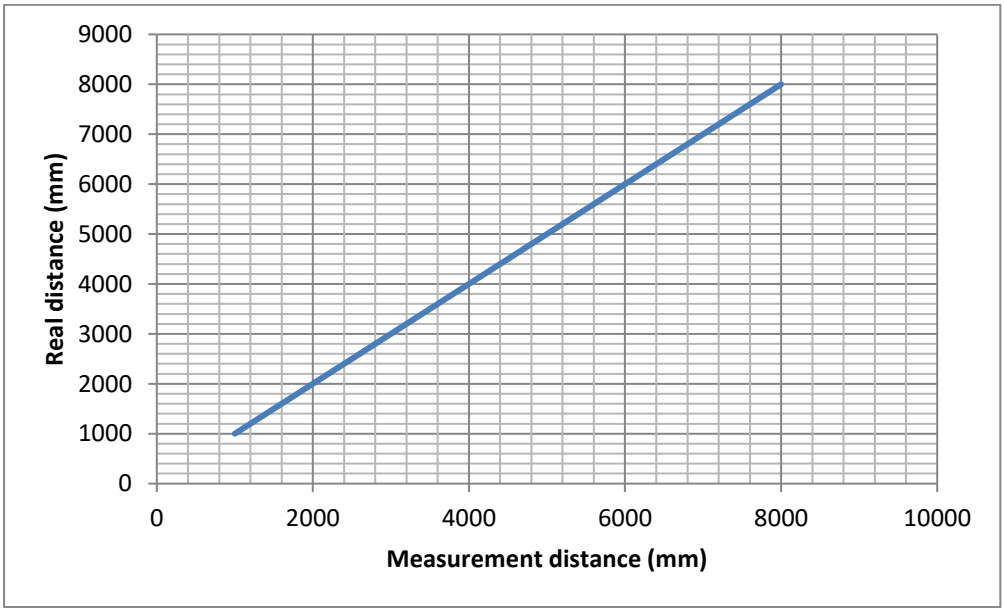

Figure 5: Measuring position from subjective view.

5. Conclusion

We built a device to detect the location and attitude of such an automated robot in the study. This has a relatively simple configuration that uses laser projecting pointers and cameras. Picture software estimated the location and attitude of the cameras and mobile robot by photographing a targeted architecture and projecting laser pointers. We looked at the number of laser pointers that were required and tested this strategy. The findings of the research are summarized here. (1) The highest location inaccuracy was 2.8 percent while measuring location by object view. As in a range of firing distances ranging 1000 mm to 4000 mm, such a system could estimate location with such an inaccuracy of lower than 50 mm. (2) As in subject view attitude evaluation, whenever xc1 and yc1 were altered, the highest error was 0.5 and 6.6 degrees respectively as well as while the xc1 and yc1 were altered, the highest error around xc1 axis will be 2.6 degrees. They are precise enough for distances of lower than 300 mm. (3) The system's principle can be adapted to a larger size robotic system with improved GPS accuracy as well as barrier mitigation systems like visual and laser proximity detectors.

REFERENCE

1. Lino Marques. “Mobile pneumatic robot for demining”, Proceedings of the 2002 IEEE International Conference on Robotics & Automation Washington, May 2002 pp 3508-3513.
2. Richard W. Wall “Creating a low-cost autonomous vehicle”, IECON 02 [Industrial Electronics Society, IEEE 2002 28th Annual Conference of the IEEE], 5-8 Nov. 2002 pp 3112- 3116.
3. Isobe, Y.; Masuyama, G.; Umeda, K. Target tracking for a mobile robot with a stereo camera considering illumination changes. In Proceedings of the IEEE/SICE International Symposium on System Integration, Nagoya, Japan, 11–13 December 2015; pp. 702–707.
4. Kawanishi, R.; Yamashita, A.; Kaneko, T.; Asama, H. Parallel line-based structure from motion by using omnidirectional camera in textureless scene. Adv. Robot. 2013, 27, 19–32.
5. Singh, T.R.; Roy, S.; Singh, O.I.; Sinam, T.; Singh, K.M. A new local adaptive thresholding technique in binarization. Int. J. Comput. Sci. Issues 2011, 8, 271–277.
6. Ragulskis, M.; Aleksa, A. Image hiding based on time-averaging moiré. Opt. Commun. 2009, 282, 2752–2759.
7. Oliveira, H.; Correia, P.L. Automatic Road crack segmentation using entropy and image dynamic thresholding. In Proceedings of the European Signal Processing Conference, Glasgow, UK, 24–28 August 2009; pp. 622–626.
8. Ubukata, T.; Terabayashi, K.; Mora, A.; Kawashita, T.; Masuya, G.; Umeda, K. Fast human detection combining range image segmentation and local feature-based detection. In Proceedings of the International Conference on Pattern Recognition, Stockholm, Sweden, 24–28 August 2014; pp. 4281–4286.
9. Zhou, F.; Peng, B.; Cui, Y.; Wang, Y.; Tan, H. A novel laser vision sensor for omnidirectional 3D measurement. Opt. Laser Technol. 2013, 45, 1–12.
10. Yagi, Y.; Nagai, H.; Yamazawa, K.; Yachida, M. Reactive visual navigation based on omnidirectional sensing—Path following and collision avoidance. J. Intell. Robot. Syst. 2001, 31, 379–395.
11. Yamaguchi, T.; Nakamura, S.; Saegusa, R.; Hashimoto, S. Image-based crack detection for real concrete surfaces. IEEJ Trans. Electr. Electron. Eng. 2008, 3, 128–135.
12. Hashmi, M.F.; Keskar, A.G. Computer-vision based visual inspection and crack detection of railroad tracks. Available online: http://www.inase.org/library/2014/venice/bypaper/OLA/OLA-16.pdf (accessed on 7 April 2020).

13. Zidek, K.; Hosovsky, A. Image thresholding and contour detection with dynamic background selection for inspection tasks in machine vision. Int. J. Circuits. Syst. Signal Process. 2014, 8, 545–554.
14. Prasanna, P.; Dana, K.; Gucunski, N.; Basily, B. Computer vision-based crack detection and analysis. Proc. SPIE 2012, 8345, 834542.
15. Mozos, O.M.; Kurazume, R.; Hasegawa, T. Categorization of indoor places using the Kinect sensor. Sensors 2012, 12, 6695–6711.
16. Hafnera, F.M.; Bhuiyanb, A.; Kooij, J.F.P.; Granger, E. RGB-depth cross-modal person re-identification. In Proceedings of the 16th IEEE International Conference on Advanced Video and Signal Based Surveillance 2019, Taipei, Taiwan, 18–21 September 2019; p. 8909838.
17. Henry, P.; Krainin, M.; Herbst, E.; Ren, X.; Fox, D. RGB-d mapping: Using depth cameras for dense 3D modeling of indoor environments. In Experimental Robotics; Springer: Berlin/Heidelberg, Germany, 2014; pp. 477–491.
18. Ren, J.; Gong, X.; Yu, L.; Zhou, W.; Yang, M.Y. Exploiting global priors for RGB-d saliency detection. In Proceedings of the IEEE Conference on Computer Vision and Pattern Recognition Workshops, Boston, MA, USA, 7–12 June 2015; pp. 25–32.
19. J. A. V. N. T. S. Center Vulnerability assessment of the transport infrastructure relying on the global positioning system. Office of the Assistant Secretary for Transportation Policy, U.S. Department of Transportation, Report, Aug. 2001.
20. Kaiser, K., Gans, N., and Dixon, W. Position and orientation an aerial vehicle through chained, vision-based pose reconstruction. In Proceedings of the AIAA Conference on Guidance, Navigation and Control, 2005.
21. Kaiser, K., Gans, N., and Dixon, W. Localization and control an aerial vehicle through chained, vision-based pose reconstruction. In Proceedings of the American Control Conference, 2007, 5934—5939.
22. Hu, G., Mehta, S., Gans, N., and Dixon, W. E. Daisy chaining based visual servo control. Part I: Adaptive quaternion-based tracking control. In Proceedings of the IEEE Multi-conference on Systems and Control, 2007, 1474—1479.
23. Hu, G., Gans, N., Mehta, S., and Dixon, W. E. Daisy chaining based visual servo control. Part II: Extensions, applications and open problems. In Proceedings of the IEEE Multi-conference on Systems and Control, 2007, 729—734.
24. Chatterji, G., Menon, P., and Sridhar, B. GPS/machine vision navigation system for aircraft. IEEE Transactions on Aerospace and Electronic Systems, 33, 3 (July 1997), 1012—1025.
25. Roberts, J. M., Corke, P. I., and Buskey, G. Low-cost flight control system for a small autonomous helicopter. In Proceedings of the Australasian Conference on Robotics and Automation, 2002.
26. Zhang, H. and Ostrowski, J. Visual servoing with dynamics: Control of an unmanned blimp. In Proceedings of the IEEE International Conference on Robotics and Automation, vol. 1, May 1999, 618—623.
27. Suresh, P., Rajesh, K.B. and Sivasubramonia Pillai, T.V. and Jaroszewicz, Z., “Effect of annular obstruction and numerical aperture in the focal region of high NA objective lens,” Elsevier – Optics Communication, Vol – 318, 2014, pp. 137–141.
28. Jones, C. G., Heyder-Bruckner, J. F., Richardson, T. S., and Jones, D. C. Vision-based control for unmanned rotorcraft. In Proceedings of the AIAA Guidance, Navigation, and Control Conference, 2006.
29. Saripalli, S., Montogomery, J. F., and Sukhatme, G. S. Visually guided landing of an unmanned aerial vehicle. IEEE Transactions on Robotics and Automation, 19, 3 (2003), 371—380.

30. chatterji, G. B., Menon, P. K., and Sridhar, B. Vision-based position and attitude determination for aircraft night landing. Journal of Guidance, Control, and Dynamics, 21, 1 (1998), 84—92.
31. Suresh, P., Thilagavathi. R., Gokulakrishnan, K., Rajesh, K.B. and Pillai, T.V.S., "Focusing properties of a 4Pi configuration system under the illumination of double ring shaped LG11 beam," Springer – Optical and Quantum Electronics, 1-6, 2014
32. Shakernia, O., Ma, Y., Koo, T. J., and Sastry, S. Landing an unmanned air vehicle: Vision based motion estimation and non-linear control. Asian Journal of Control, 1 (1999), 128—145.
33. Yakimenko, O., Kaminer, I., Lentz, W., and Ghyzel, P. Unmanned aircraft navigation for shipboard landing using infrared vision. IEEE Transactions on Aerospace and Electronic Systems, 38, 4 (Oct. 2002) 1181—1200.
34. Suresh, P., Mariyal, C., Rajesh, K.B. and Pillai, T.V.S., "Polarization effect of cylindrical vector beam in high numerical aperture lens Axicon systems," Elsevier – Optik, Vol. 124, 2013. pp. 1632-1636
35. Jianchao, Y. A new scheme of vision-based navigation for flying vehicles–concept study and experiment evaluation. In Proceedings of the IEEE International Conference on Control, Automation, Robotics And Vision, 2002, 643—648.
36. Barber, D. B., Griffiths, S. R., McLain, T. W., and Beard, R. W. Autonomous landing of miniature aerial vehicles. Journal of Aerospace Computing, Information, and Communication, 4 (2007), 770.
37. Bryson, M. and Sukkarieh, S. Observability analysis and active control for airborne SLAM. IEEE Transactions on Aerospace and Electronic Systems, 44, 1 (Jan. 2008), 261—280.
38. Kim, J. and Sukkarieh, S. Autonomous airborne navigation in unknown terrain environments. IEEE Transactions on Aerospace and Electronic Systems, 40, 3 (July 2004), 1031—1045.
39. Trisiripisal, P., Parks, M. R., Abbot, A. L., Liu, T., and Fleming, G. A. Stereo analysis for vision-based guidance and control of aircraft landing. Presented at the AIAA Aerospace Sciences Meeting and Exhibit, 2006.
40. Wu, A. D., Johnson, E. N., and Proctor, A. A. Vision-aided inertial navigation for flight control. Journal of Aerospace Computing, Information, and Communication, 2 (2005), 348—360.
41. Suresh, P., Mariyal, C., Gokulakrishnan, K., Rajesh, K.B. and Pillai, T.V.S., "Tight Focusing of Circularly Polarized Beam over high NA Lens Axicon with a Diffractive Optical Element," Elsevier – Optik, vol. 124. Issue 20, 2013. pp. 4389-4392
42. Caballero, F., Merino, L., Ferruz, J., and Ollero, A. Improving vision-based planar motion estimation for unmanned aerial vehicles through online mosaicing. In Proceedings of the IEEE International Conference on Robotics and Automation, 2006, 2860—2865.